Journal of Magnetic Resonance **148,** 209–213 (2001)
doi:10.1006/jmre.2000.2234, available online at http://www.idealibrary.com on IDEAL®

COMMUNICATIONS

Sensitivity Enhancement of a Two-Dimensional Experiment for the Measurement of Heteronuclear Long-Range Coupling Constants, by a New Scheme of Coherence Selection by Gradients

Daniel O. Cicero, Gaetano Barbato, and Renzo Bazzo[1]

Istituto di Ricerche di Biologia Molecolare P. Angeletti, Via Pontina km 30.600, 00040 Pomezia, Rome, Italy

Received May 18, 2000; revised September 6, 2000

In this work we present a new pulse sequence for the measurement of long-range heteronuclear coupling constants in which the optimization of coherence selection by pulsed field gradients offers a net increase in sensitivity. This type of experiments is extremely valuable for conformational studies of molecules in natural abundance and in this context the use of gradients is essential for an efficient suppression of ^{12}C bound proton signals. A comparative analysis of the different gradient schemes available is presented with a conclusive elucidation of the relative sensitivities. Our gradient scheme could be advantageous as a building block for other related experiments. © 2001 Academic Press

Key Words: **HMBC; long-range heteronuclear couplings; gradient spectroscopy.**

Heteronuclear correlations and corresponding coupling constants, especially ^{1}H–^{13}C coupling constants, are recognized as valuable parameters in assessing the conformation and structure of molecules in solution (*1*). In the specific case of the conformational analysis of nucleosides in solution, the combined use of ^{1}H–^{13}C and ^{1}H–^{1}H couplings greatly improves the level of accuracy that can be obtained for the conformation of the sugar ring, as was already demonstrated in the case of 3′-azido-3′-deoxythymidine (AZT) (*2*).

A number of different approaches have been used for the measurement of these parameters, including experiments like the HECADE (*3, 4*), HETLOC (*5, 6*), HSQMBC (*7*), GSQMBC (*8–10*), HMBC (*11–14*), and Accordion-optimized experiments (*15*).

A very convenient way of measuring heteronuclear coupling constants in natural abundance is the use of the two-dimensional heteronucleus-coupled ω_1 hetero-half-filtered proton–proton correlation (HETLOC) (*5, 6*). A more recent 1D version of this technique was developed in our laboratory (*16*). These experiments provide coupling constants only for fragments of the type H–C–C(H)–C–H. On the other hand, experiments based on the standard heteronuclear multiple-bond correlation (HMBC) technique (*17*) are of more general applicability, since they provide values for coupling constants among protons and all classes of carbons, including quaternary carbons.

The first approach to render the original HMBC useful for the measurement of the heteronuclear coupling was described by Titman *et al.* in 1989 (*18*). This experiment uses a phase-sensitive 2D HMBC pulse sequence (Fig. 1A) and a reference 1D spectrum collected to provide the phase correction necessary for the extraction of the long-range coupling values from the corresponding multiple-bond correlation peaks. Indeed, the internal multiplet structure of such cross peaks is in general rather complex due to a large phase modulation arising from proton shifts and proton–proton coupling evolution during the long fixed delay necessary to build up the multiple-bond correlation. In order to extract the value of such long-range couplings, a fitting procedure has been devized (*18*), whereby an accurate model is used to represent both the phase modulation and the antiphase structure. In a subsequent paper (*19*), the authors examined how the accuracy of the coupling constant values measured by this method were affected both by systematic deviations of the data from the theoretical assumptions and by random errors.

The basic assumption of the method described above is the possibility of generating, by calculation from a simple proton spectrum, multiplets with *precisely* the same phase distortions due to the evolution of proton shifts and couplings as found in the two-dimensional spectrum. More recently, Sheng and van Halbeek have proposed an elegant procedure for obtaining these *reference multiplets* (*12*) without the need of any extra data or calculation. They observed that if no suppression of one-bond correlations is performed, one can use the corresponding $^{1}J_{CH}$ correlation peaks as reference, as the two "satellite" lines have the same phase properties since they are collected under identical experimental conditions.

A second contribution of the authors to this method was the introduction of pulsed field gradients (PFG) to obtain a better suppression of the strong signal arising from protons attached

[1] To whom correspondence should be addressed. Fax: 39-06-91093-225. E-mail: bazzo@irbm.it.

1090-7807/01 $35.00

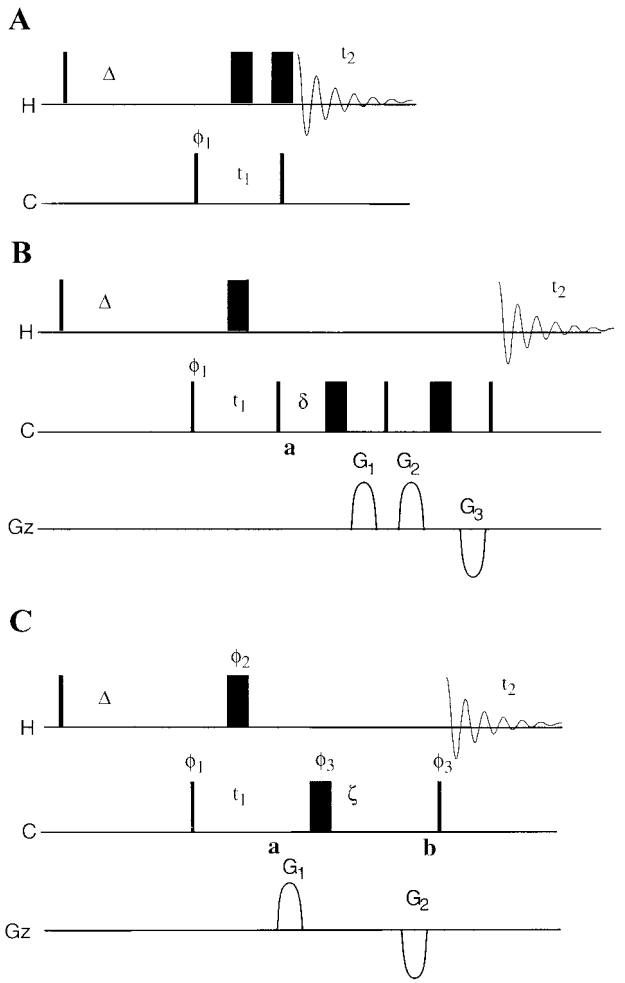

FIG. 1. Pulse sequences of the phase-sensitive HMBC. The delay Δ is for H–C long-range coupling evolution, typically on the order of 40 to 60 ms. (A) Phase-sensitive 2D HMBC, without gradient selection (*18*). (B) Gradient-enhanced 2D HMBC with gradient selection after quadrature detection (*12*). Quadrature detection is accomplished by incrementing ϕ_1 via the States–TPPI method (*29*). Delay δ is calculated to center the subsequent 180° pulse on C with respect to the two flanking 90° pulses. The gradient ratio used is $G_1{:}G_2{:}G_3 = 4{:}3{:}-5$. (C) Phase-sensitive HMBC with echo–antiecho quadrature detection proposed in this work. Even and odd transients are stored in separate memory locations for later recombination to afford fully phase-sensitive data. The following phase cycling is applied: $\phi_1 = x, -x$; $\phi_2 = x, x, -x, -x$; $\phi_3 = 4x, 4(-x)$; $\phi_R = x, -x, x, -x, -x, x, -x, x$. Gradient ratios: $G_1{:}G_2 = 5{:}-3$ (odd experiments) and $3{:}-5$ (even experiments). Delay ζ is set to guarantee no ^{13}C chemical shift evolution for the first value of t_1, thereby producing a 0,0 phase correction in F_1. Its value is calculated as $\zeta = (t_1)_0 + p_{180H}$, where $(t_1)_0$ is the initial value of t_1, and p_{180H} is the duration of the proton 180° pulse.

to ^{12}C nuclei, leading to a significant reduction in t_1 noise. There are at least three different methods for the use of PFG for the selection of the coherence transfer pathways that involve ^{13}C, and produce at the same time pure-absorption lineshapes in the t_1 dimension. The switched acquisition time (SWAT) method employs gradients during acquisition (*20*). The second method combines a conventional quadrature detection in t_1 (for example, using the States–TPPI recipe), with a subsequent gradient selection of only one of the two coherence pathways (*21*), and it is the one proposed by Sheng and van Halbeek (Fig. 1B). The third method involves the use of gradients also in the quadrature detection, by combining two experiments that select alternatively the $p = 1$ or the $p = -1$ coherence pathways. The combination of these two experiments yields a pure-absorption lineshape in t_1 (*22*).

Although these two latter gradient selection methods were presented as equivalent (*12*), the last one proves to be more sensitive. Therefore, on this basis we propose a new pulse sequence (Fig. 1C) that improves by a factor of $\sqrt{2}$ the sensitivity of pulse sequence 1B.

In the pulse sequence of Fig. 1B, the gradient selection can be considered an addendum to the original phase-sensitive HMBC 1A. It is clear that the intensity of the cosine- or sine-modulated terms of the quadrature in t_1, generated by changing the phase ϕ in the odd or even experiments, respectively, is diminished by a factor of 2 by the gradient selection of only one of the two pathways. This leads to an overall loss in S/N of a factor of 2 when comparing sequences 1B and 1A.

On the other hand, both the cosine- and the sine-modulated terms are detected in the odd or even experiments when pulse sequence 1C is used (see Appendix), with a reduction by half of their intensity due to the gradient selection. The combination of the two experiments, with a phase shift of 90° of the even experiments, yields a pure-absorption lineshape in t_1, where the signal intensity is the same as that in 1A (and thus double with respect to 1B). However, as we obtain this result by summing two experiments, the noise is increased by a factor of $\sqrt{2}$, thereby leading to a reduction of $\sqrt{2}$ in S/N when compared with sequence 1A, but with an identical gain with respect to sequence 1B. Similar arguments have earlier been proposed for the application of gradients to the three-dimensional HNCO experiment (*23*).

Two experiments, using sequences 1B and 1C, were recorded using identical conditions on a solution of AZT in DMSO as test sample. Figure 2 shows the 2D spectrum obtained using sequence 1C, and the arrow indicates the trace extracted to compare the relative sensitivity of the two experiments. The two traces are shown in Fig. 3, where the direct $^1J_{HC}$ correlation between H-1′ and C-1′ is shown together with the long-range $^3J_{HC}$ correlation between H-1′ and C-4′ (central multiplet), since C-1′ and C-4′ have virtually identical chemical shifts. Traces I and II correspond to the application of sequences 1B and 1C, respectively. As expected, the signal intensity is doubled when applying pulse sequence 1C, whereas the noise is increased by a factor of $\sqrt{2}$ (see Fig. 3). The resulting experimental S/N is almost identical to the theoretical value ($62/44 \approx 1.41$).

Additionally, one should appreciate that sequence 1C contains fewer pulses than 1B, and therefore it is less sensitive to RF pulse imperfections.

Finally, it is important to point out that the application of the method developed by Rance and Lewis (*24–26*), although convenient in many experiments, can hardly be expected to

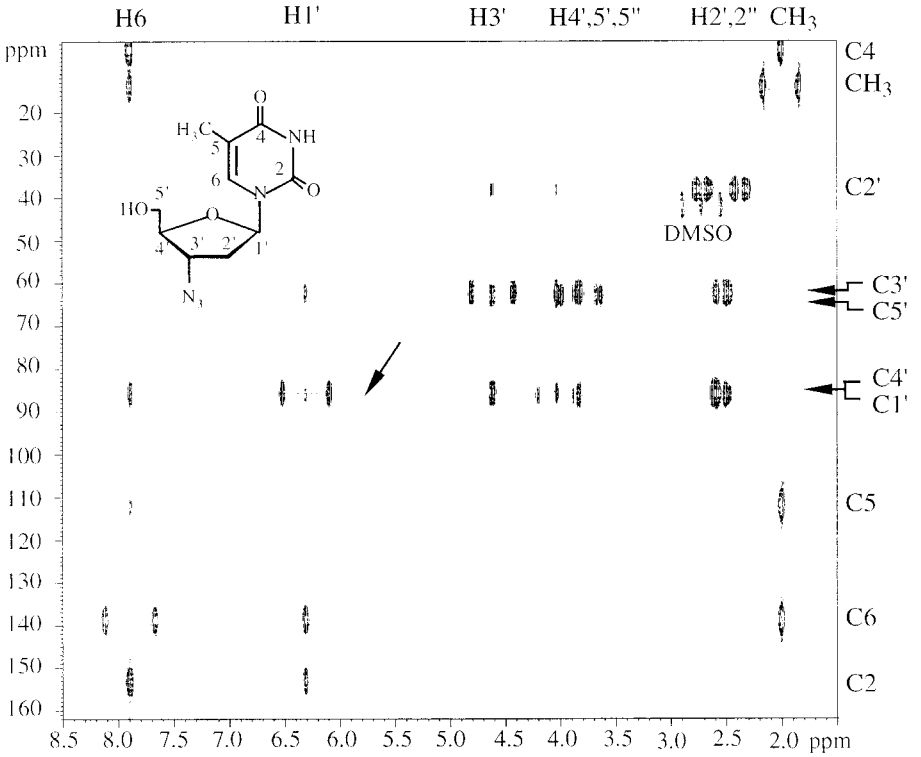

FIG. 2. 2D HMBC spectrum of a 50 mM 3′-azido-3′-deoxythymidine (AZT) sample in DMSO-d_6, recorded at 500 MHz and 25°C on a Bruker Avance spectrometer equipped with a *z*-shielded gradient triple-resonance probe, and using the pulse sequence 1C. The delay Δ was set to 48.28 ms and the acquisition times t_2 and t_1 were 1.3 s (spectral width 6410 Hz, 8K complex data points) and 3 ms (spectral width 20,100 Hz, 64 real data points), respectively. The relaxation delay was 2 s; 80 scans were accumulated per t_1 increment. Sine-bell gradient pulses of 1 ms duration were used; *z* gradients G_1 and G_2 were 25 and 15 G/cm, respectively. The total acquisition time was approximately 6 h. The arrow indicates the trace used for sensitivity comparison in Fig. 3. C-4 is folded in the present experiment.

improve sensitivity in this particular case since it requires the refocusing of the corresponding heteronuclear coupling constants. This is perfectly feasible only for IS spin systems leading to a gain in *S*/*N* of 2 compared to sequences like 1C, or $2\sqrt{2}$ with respect to sequence 1B. However, a fast inspection of Fig. 2 will suffice to realize that most of the spin systems are of the I_nS type, with *n* ranging from 2 to 6, or even more, since in this case *n* represents the number of protons that are one, two, or three bounds removed from a given carbon. An extra complication comes from the fact that all the coupling constants are in principle different, spanning values as different as 1 to 11 Hz. Clearly, as shown by Griesinger and co-workers (*27*) the refocusing is still at least partially feasible for systems like the directly coupled CH, CH_2, and CH_3 groups, with the direct coupling constants of similar known magnitude. For long-range unknown coupling constants simply the trick does not apply.

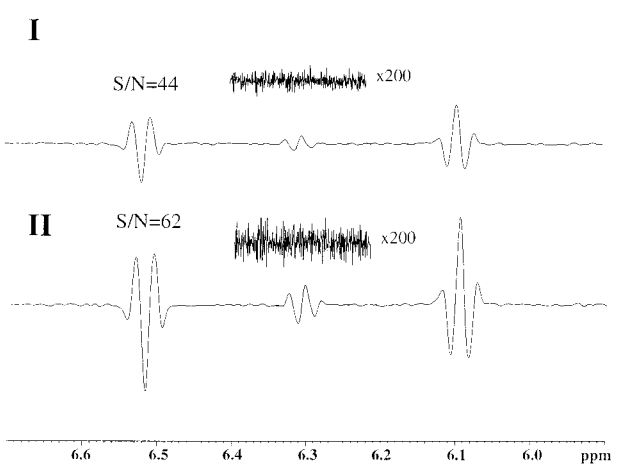

FIG. 3. Rows of the 2D experiments performed using sequences 1B (trace I) and 1C (trace II). The rows were obtained at the chemical shift of carbons 1′ and 4′ (see Fig. 2). Both experiments were performed using identical conditions.

In conclusion, the only possible sensitivity enhancement of the experiment proposed by Sheng and van Halbeek (*12*) is represented by our scheme (sequence 1C). One should appreciate that the echo–antiecho quadrature detection is here implemented by employing only two gradients, whereas three gradients are commonly used. The difference here is that with two gradients one needs, in alternate scans, to swap the gradient absolute intensities while keeping the same sign (see the legend to Fig. 1), whereas with three gradients one need just reverse the sign of one. In this case with a marginally more

articulate use of just two gradients one avoids the introduction of a third one that would necessarily impose an extra delay. Therefore also in other pulse sequences one could find the use of our scheme more convenient than the conventional one.

A detailed description of the experiments, with particular attention to the coherence evolution induced by gradients, is reported in the Appendix, using the product operator formalism (*28*).

APPENDIX

Let us consider a three-spin system consisting of two protons I_1 and I_2, and a carbon-13 nucleus S, where the two protons are coupled with a coupling of J_H, I_1 is coupled to S with a coupling J_{IS}, and I_2 is not coupled to S. This system is sufficient to illustrate the phase modulation and the relative sensitivity of the sequences depicted in Fig. 1.

Sequence 1B

The first part of the sequence is identical to that already described by Titman *et al.* (*18*), with quadrature detection in t_1 by changing phase ϕ_1. At point *a* the magnetization can be described by (*18*)

$$\rho_a = \sin(\pi J_{IS}\Delta)\cos(\Omega_S t_1)[-c_H c_1 2I_{1x}S_z - c_H s_1 2I_{1y}S_z + s_H s_1 4I_{1x}I_{2z}S_z - s_H c_1 4I_{1y}I_{2z}S_z], \quad [1]$$

where

$$c_H = \cos(\pi J_H\Delta), \quad s_H = \sin(\pi J_H\Delta),$$
$$c_1 = \cos(\Omega_1\Delta), \quad s_1 = \sin(\Omega_1\Delta).$$

Next, we apply the gradient selection. We can derive the expression for each one of the four terms in [1], and we will calculate the gradient refocusing condition by obtaining the expression for the first term ($2I_{1x}S_z$). This term is converted by the subsequent pulses and gradients to

$$-\frac{i}{2}[I_1^+S^-\exp(-i\theta_a) - I_1^+S^+\exp(-i\theta_b) + I_1^-S^-\exp(i\theta_b) - I_1^-S^+\exp(i\theta_a)], \quad [2]$$

where

$$\theta_a = \gamma_1 G_1 + (\gamma_I + \gamma_S)G_2 + (\gamma_I - \gamma_S)G_3,$$
$$\theta_b = \gamma_I G_1 + (\gamma_I - \gamma_S)G_2 + (\gamma_I + \gamma_S)G_3,$$

$G_i = B_{1(z)i}\tau_i$ is the product of the gradient strength by the gradient duration, and γ_I and γ_S are the gyromagnetic ratios of proton and carbon, respectively. Then one can choose a gradient combination that makes either θ_a or θ_b zero (but not both). With $\theta_a = 0$ one can deduce the following transformation produced by the gradient selection:

$$2I_xS_z \rightarrow -\frac{1}{2}(2I_xS_z). \quad [3]$$

A similar result can be deduced for the other three terms within [1], yielding the following expressions for the two separate experiments:

odd experiments ($\phi_1 = x$):

$$\tfrac{1}{2}\sin(\pi J_{IS}\Delta)\cos(\Omega_S t_1)[A] \quad [4]$$

even experiments ($\phi_1 = y$):

$$\tfrac{1}{2}\sin(\pi J_{IS}\Delta)\sin(\Omega_S t_1)[A], \quad [5]$$

where

$$A = -c_H c_1 2I_{1x}S_z - c_H s_1 2I_{1y}S_z + s_H s_1 4I_{1x}I_{2z}S_z - s_H c_1 4I_{1y}I_{2z}S_z.$$

Cross peaks are obtained with an absorption-mode lineshape in F_1 (the cosine- and sine-modulated terms are separate), and with a complex superposition of lines of all phases in F_2. If compared to the standard quadrature-detected experiments without the use of gradients a factor of 2 in sensitivity is formally lost.

Sequence 1C

At point *a* the density operator has the form

$$\rho_a = \sin(\pi J_{IS}\Delta)\cos(\Omega_S t_1)[-c_H c_1 2I_{1x}S_y - c_H s_1 2I_{1y}S_y + s_H s_1 4I_{1x}I_{2z}S_y - s_H c_1 4I_{1y}I_{2z}S_y] - \sin(\pi J_{IS}\Delta)\sin(\Omega_S t_1)[-c_H c_1 2I_{1x}S_x - c_H s_1 2I_{1y}S_x + s_H s_1 4I_{1x}I_{2z}S_x - s_H c_1 4I_{1y}I_{2z}S_x]. \quad [6]$$

As in the precedent case, we will derive the expression at point *b* for the first term of each bracket in [6]. It can be easily calculated that these two terms are transformed into

$$2I_{1x}S_y \rightarrow \frac{1}{2i}[I_1^+S^-\exp(-i\theta_1) - I_1^+S^+\exp(-i\theta_2) + I_1^-S^-\exp(i\theta_2) - I_1^-S^+\exp(i\theta_1)] \quad [7]$$

$$2I_{1x}S_x \rightarrow \frac{1}{2}[I_1^+S^-\exp(-i\theta_1) + I_1^+S^+\exp(-i\theta_2) + I_1^-S^-\exp(i\theta_2) + I_1^-S^+\exp(i\theta_1)], \quad [8]$$

where

$$\theta_1 = (\gamma_I + \gamma_S)G_1 + (\gamma_I - \gamma_S)G_2,$$
$$\theta_2 = (\gamma_I - \gamma_S)G_1 + (\gamma_I + \gamma_S)G_2.$$

In this case we will perform two separate experiments. The odd experiments will have a ratio $G_1{:}G_2$ so as to make $\theta_1 = 0$. The even experiments will make $\theta_2 = 0$. This can be readily achieved by using the following gradient ratios:

$$\text{odd experiments:} \quad G_1{:}G_2 = 5{:}-3$$
$$\text{even experiments:} \quad G_1{:}G_2 = 3{:}-5.$$

Using these two conditions, we can calculate the final form of these two operators in both experiments, just before detection:

odd experiments ($\theta_1 = 0$):

$$2I_{1x}S_y \rightarrow -\tfrac{1}{2}(2I_{1x}S_z), \quad 2I_{1x}S_x \rightarrow -\tfrac{1}{2}(2I_{1y}S_z) \qquad [9]$$

even experiments ($\theta_2 = 0$):

$$2I_{1x}S_y \rightarrow -\tfrac{1}{2}(2I_{1x}S_z), \quad 2I_{1x}S_x \rightarrow +\tfrac{1}{2}(2I_{1y}S_z). \qquad [10]$$

This result can be extended to the remaining terms in [6], producing the following expression for the observable magnetization:

odd experiments ($\theta_1 = 0$):

$$-\tfrac{1}{2}\sin(\pi J_{IS}\Delta)\cos(\Omega_S t_1)[A] + \tfrac{1}{2}\sin(\pi J_{IS}\Delta)\sin(\Omega_S t_1)[\bar{A}] \qquad [11]$$

even experiments ($\theta_2 = 0$):

$$-\tfrac{1}{2}\sin(\pi J_{IS}\Delta)\cos(\Omega_S t_1)[A] - \tfrac{1}{2}\sin(\pi J_{IS}\Delta)\sin(\Omega_S t_1)[\bar{A}], \qquad [12]$$

where A has the same meaning as in [4], and $\bar{A}$ represents the same operators but with a 90° phase difference for I_1.

As already described (*26*), the processing recipe that produces a phase-sensitive spectrum implies the sum and the difference of the two experiments and a 90° phase correction of each second experiment, to yield

$$\sin(\pi J_{IS}\Delta)\cos(\Omega_S t_1)[A] \quad \text{(sum)} \qquad [13]$$
$$\sin(\pi J_{IS}\Delta)\sin(\Omega_S t_1)[A] \quad \text{(difference)}. \qquad [14]$$

By comparing [13] with [4] and [14] with [5], one can easily recognize the gain factor of 2 in signal intensity, although, as we have obtained this result by combining two experiments, the noise is also increased by a factor of $\sqrt{2}$. In conclusion, the final gain in signal/noise is, as it turns out, precisely $\sqrt{2}$.

REFERENCES

1. J. L. Marshall, "Carbon–Carbon and Carbon–Proton NMR Couplings: Application to Organic Stereochemistry and Conformational Analysis," Verlag Chemie International, Florida (1983).
2. D. O. Cicero, G. Barbato, and R. Bazzo, *Tetrahedron* **51,** 10303–10316 (1995).
3. W. Kozminski and D. Nanz, *J. Magn. Reson.* **142,** 294–299 (2000).
4. W. Kozminski and D. Nanz, *J. Magn. Reson.* **124,** 383–392 (1997).
5. D. Uhrin, G. Batta, V. J. Hruby, P. N. Barlow, and K. E. Kover, *J. Magn. Reson.* **130,** 155–161 (1998).
6. M. Kurtz, P. Schmieder, and H. Kessler, *Angew. Chem. Int. Ed. Engl.* **30,** 1329–1331 (1991).
7. R. T. Williamson, B. L. Marquez, W. H. Gerwick, and K. E. Kover, *Magn. Reson. Chem.* **38,** 265–273 (2000).
8. R. Marek, L. Kralik, and V. Sklenar, *Tetrahedron Lett.* **38,** 665–668 (1997).
9. R. Marek, *Collect. Czech. Chem. Commun.* **62,** 1747–1753 (1997).
10. K. Furihata and H. Seto, *Tetrahedron Lett.* **40,** 6271–6275 (1999).
11. G. Zhu, A. Renwick, and A. Bax, *J. Magn. Reson.* **110,** 257–261 (1994).
12. S. Sheng and H. van Halbeek, *J. Magn. Reson.* **130,** 296–299 (1998).
13. W. Wilker and D. Leibfritz, *Magn. Reson. Chem.* **33,** 632–638 (1995).
14. K. Ding, *Magn. Reson. Chem.* **38,** 321–323 (2000).
15. C. H. Gotfresen, A. Meissner, J. O. Duus, and O. W. Sørensen, *Magn. Reson. Chem.* **38,** 692–695 (2000).
16. R. Bazzo, G. Barbato, and D. O. Cicero, *J. Magn. Reson. A* **117,** 267–271 (1995).
17. A. Bax and M. F. Summers, *J. Am. Chem. Soc.* **108,** 2093–2094 (1986).
18. J. J. Titman, D. Neuhaus, and J. Keeler, *J. Magn. Reson.* **85,** 111–131 (1989).
19. J. M. Richardson, J. J. Titman, J. Keeler, and D. Neuhaus, *J. Magn. Reson.* **93,** 533–553 (1991).
20. R. E. Hurd, B. K. John, and H. D. Plant, *J. Magn. Reson.* **93,** 666–670 (1991).
21. G. W. Vuister, J. Ruiz-Cabello, and P. C. M. van Zijl, *J. Magn. Reson.* **100,** 215–220 (1992).
22. A. L. Davis, J. Keeler, E. D. Laue, and D. Moskau, *J. Magn. Reson.* **98,** 207–216 (1992).
23. J. Schleucher, M. Sattler, and C. Griesinger, *Angew. Chem. Int. Ed. Engl.* **32,** 1489–1491 (1993).
24. J. Cavanagh, A. G. Palmer, III, P. E. Wright, and M. Rance, *J. Magn. Reson.* **91,** 429–436 (1991).
25. A. G. Palmer, III, J. Cavanagh, P. E. Wright, and M. Rance, *J. Magn. Reson.* **93,** 151–170 (1991).
26. L. E. Kay, P. Keifer, and T. Saarinen, *J. Am. Chem. Soc.* **114,** 10663–10665 (1992).
27. J. Schleucher, M. Schwendinger, M. Sattler, P. Schmidt, O. Schedletzky, S. J. Glaser, O. W. Sørensen, and C. Griesinger, *J. Biomol. NMR* **4,** 301–306 (1994).
28. O. W. Sørensen, G. W. Eich, M. H. Levitt, G. Bodenhausen, and R. R. Ernst, *Prog. NMR Spectrosc.* **16,** 163 (1983).
29. D. Marion, M. Ikura, R. Tschudin, and A. Bax, *J. Magn. Reson.* **85,** 393–399 (1989).